A Triple-Band Absorber with Wide Absorption Bandwidths Using Impedance Matching Theory

Mei, Peng; Zhang, Shuai; Lin, Xianqi; Pedersen, Gert F.

Published in:
IEEE Antennas and Wireless Propagation Letters

DOI (link to publication from Publisher):
10.1109/LAWP.2019.2895971

Publication date:
2019

Document Version
Accepted author manuscript, peer reviewed version

This article has been accepted for publication in a future issue of this journal, but has not been fully edited. Content may change prior to final publication. Citation information: DOI 10.1109/LAWP.2019.2895971, IEEE Antennas and Wireless Propagation Letters

A Triple-Band Absorber with Wide Absorption Bandwidths Using Impedance Matching Theory

Peng Mei, *Student Member, IEEE*, Shuai Zhang, *Senior Member, IEEE*, Xian Qi Lin, *Senior Member, IEEE*, and Gert Frølund Pedersen, *Senior Member, IEEE*

***Abstract*—This letter presents multi-band absorbers with wide absorption bandwidths based on impedance matching theory. A wideband absorber with good absorption performance is served as a matching load for multi-band bandpass frequency selective surface (FSS) filters. As a result, the reflection coefficients of the proposed absorbers are in high accordance with the counterparts of the original bandpass FSS filters. For demonstration, a triple-band absorber with wide absorption bandwidths is designed and fabricated by cascading a triple-band bandpass FSS filter and wideband absorber together. The simulated results reveal that the proposed absorber has wide fractional bandwidths of 5.2 %, 8.0 %, and 6.4%, which is experimentally validated by the measured results.**

***Index Terms*—Electromagnetic absorber, bandpass filter, frequency selective surfaces, impedance matching.**

I. Introduction

METAMATERIAL (MTM) absorbers have their unique advantages over conventional absorbing materials, such as, wide absorption bandwidth, low profile, easy to be assembled with antennas to improve the performance of antennas. Since the first emergence of the perfect metamaterial absorber by Landy [1], researches about MTM absorbers have been widely carried out and mainly focused on wideband absorbers [2], [3], polarization insensitivity absorbers [4],[5], wide incident angle absorbers [6],[7], multi-band absorbers [8]-[12], and band-notched absorbers [13], [14]. To realize a wideband absorption, lumped resistors are usually used to increase the real part of the input impedance of the absorber structure to make it match well with the impedance of free space (120π) in a wide frequency band [2], [3]. Some absorber unit cells with highly symmetrical patterns are proposed and employed to establish polarization insensitivity and wide incident angle absorbers [4]-[7]. For multi-band absorbers [8]-[12], a straightforward approach is utilized that multiple metallic resonators with different sizes are arranged. These absorbers can be very thin since the absorption performance and frequency is determined by the dimensions of metallic patterns or periodicity of the unit cells. However, due to the resonant characteristics of these multi-band absorbers, the bandwidth of every absorption band is extremely narrow. And the bandwidths are difficult to improve by simply increasing the supporting substrate thickness.

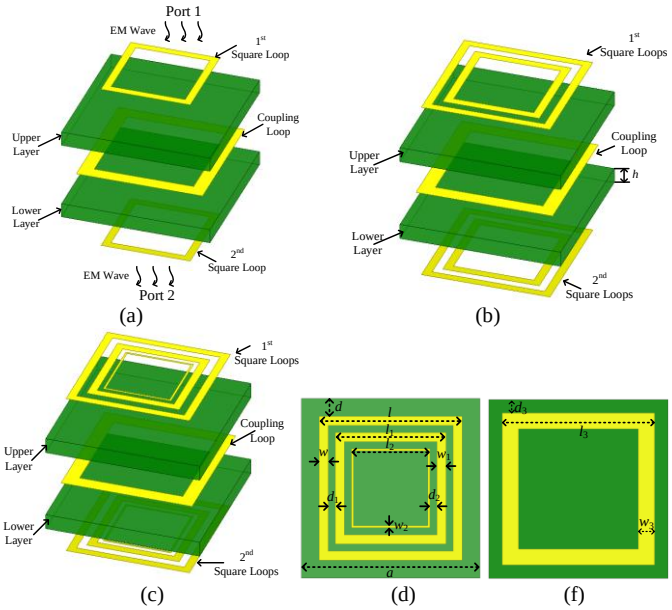

Fig. 1. Geometries of the multi-band bandpass filters based on FSS. (a). Perspective view of one passband filter. (b). Perspective view of two passbands filter. (c). Perspective view of three passbands filter. (d). Front view of 1st square loop of three passbands filter. (f). Front view of the coupling loop of three passbands filter.

In this letter, multi-band absorbers with wide absorption bandwidths are proposed based on impedance matching theory. It is required that a wideband absorber with good absorption performance is regarded as a matching load for multi-band bandpass frequency selective surface (FSS) filters. To prove the concept, three bandpass FSS filters (with single/dual/triple passbands) and a dual-polarized wideband absorber are simulated and studied individually. The proposed absorbers are then constructed by cascading the wideband absorber and FSS filters. Their reflection coefficients are simulated that are in high accordance with the counterparts of the original FSS filters. Finally, the proposed triple-band absorber is fabricated and measured. The measured and simulated results are in good agreement. The novelty of this paper is to introduce a concept which can easily realize multiple wide absorption bandwidths.

Manuscript received Nov, 2018. This work was supported in part by National Natural Science Foundation of China under Grant 61571084, in part by EPRF under Grant 6141B06120101 and AAU Young Talent program.

P. Mei, S, Zhang (Corresponding author), and G. F. Pedersen are all with the Antenna, Propagation and Millimeter-wave Section, Department of Electronic Systems, Aalborg University, Aalborg, 9000, Denmark. (email: sz@es.aau.dk)

X. Q. Lin is with the EHF Key Laboratory of Science, School of Electronic Science and Engineering, University of Electronic Science and Technology of China, Chengdu, 611731, China. (email: xqlin@uestc.edu.cn)

This article has been accepted for publication in a future issue of this journal, but has not been fully edited. Content may change prior to final publication. Citation information: DOI 10.1109/LAWP.2019.2895971, IEEE Antennas and Wireless Propagation Letters

The proposed concept for absorber designs can also be effectively generalized to a wide range of applications where arbitrary absorption responses are required, such as: multiple notch bands absorber. These properties are challenging to achieve with the previous methods, e.g., in [8]-[12]. One application of the proposed triple-band absorber is served as a functional metal ground for a multi-band antenna to achieve out-of-band radar cross section (RCS) reduction performance as explained in [13], [14].

II. Design Procedures

A. Multi-band bandpass filters design based on square loops

Three bandpass filters with one, two, and three passbands based on square loops are proposed. Fig. 1 presents the geometries of the proposed multi-band bandpass filters, which are constructed by two substrate layers. The square metallic loops are etched on the dielectric substrate with a thickness of 1 mm, a relative permittivity of 2.5, and a loss tangent of 0.002. The 1st and 2nd square loops are identical, printed on the two dielectric substrates, respectively. The intermediate square loop, sandwiched into the two substrates, serves as the coupling loop to couple the EM energy from the 1st square loop(s) to the 2nd square loop(s), resulting in EM wave transmission from port 1 to port 2. The number of passbands of the proposed filter depends on the number of 1st and 2nd square loops. The side lengths of 1st and 2nd square loops are related to the target frequency which is given by:

$$f = \frac{c}{4 \cdot l \cdot \sqrt{(\varepsilon_r + 1)/2}} \quad (1)$$

where c is the velocity in the vacuum, l is the side length of the square loop, and ε_r is the relative permittivity of the supporting dielectric substrate. High Frequency Structure Simulator (HFSS) software is utilized to carry out the full-wave simulations. Due to the highly symmetrical geometries of the proposed structure, the simulated results in one polarisation are only presented for brevity. Fig. 2 shows the S-parameters of the proposed three bandpass filters, where one, two, and three passbands are observed; their reflection phases (RP) are plotted as well.

The S-parameter of the triple-band bandpass filter is discussed. The even/odd mode theory can be used to mathematically analyze the bandpass filter [15]. For more intuitive observation, however, we analyze it from the field viewpoint. First of all, the current distributions on the square loops at reflection zero frequencies (6.73, 6.95, 9.30, 9.85, 12.86, and 13.22 GHz) are plotted in Fig. 3 (right part). Due to the identical and symmetrical geometries of the 1st and 2nd square loops, only the current distributions on the 1st square loops are given. It is observed that the current intensity on the outer/middle/inner loop is dominated at (6.75, 6.95 GHz), (9.30, 9.85 GHz), (12.86, 13.22 GHz), respectively. Half-wavelength resonances occur at these frequencies, which is highly in accordance with (1). Moreover, it can also be predicted that the first/second/third passbands can be independently tuned by modifying the dimensions of the outer/middle/inner loops, correspondingly. In order to verify the conclusions obtained from the current distribution analysis, parametric studies are carried out, where the side lengths of l ,l_1, and l_2 are independently tuned with the other parameters fixed, respectively. As shown in Fig. 3, the first passband is shifted towards higher frequencies when l reduces, because a smaller l makes the resonant frequencies increase as explained in [16], while the frequencies and bandwidths of the other two (second and third) passbands are remained. The similar results are also observed when l_1 and l_2 reduce as shown in Fig. 3. The conclusions obtained from parametric studies are highly consistent with these from the current distributions.

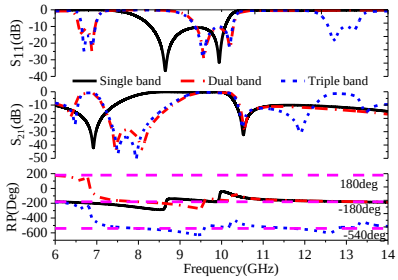

Fig. 2. S-parameters of the proposed FSS multi-band bandpass filters.

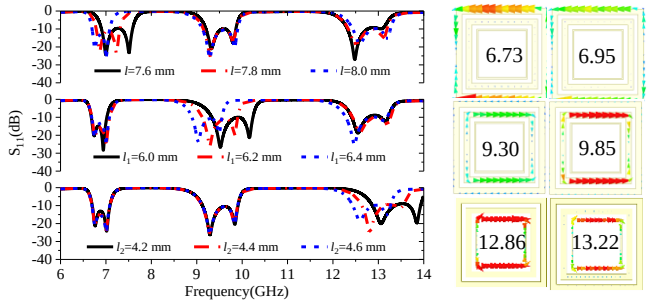

Fig. 3. S_{11} of the triple-band bandpass filter with different values of l, l_1, and l_2. (The right part is current distributions on square loop at a certain frequency, and the current scales on all loops are identical from 0 A/m to 200 A/m)

B. Dual-polarized and wideband absorber

The proposed dual-polarized and wideband absorber consists of a pair of orthogonal circular metallic patches printed on a dielectric supporting substrate, an air spacer, and a metal ground. The dielectric substrate used here is with a thickness of 1 mm, a relative permittivity of 2.5, and a loss tangent of 0.002. Four lumped resistors are soldered in the middle of these circular metallic patches as shown in Fig. 4 to achieve wideband impedance match with free space in x- and y-directions. The packaging of the lumped resistors (in Fig. 4 and Fig. 8) are 0.6 mm in length and 0.8 mm in width. The design of this kind of absorber is fully investigated in our previous work [13].

When an absorber is served as a matching load, it is usually requested that the S_{11} of the absorber is as small as possible. In order to achieve better absorption performance of the proposed absorber, some key parameters are studied. As stated before, the resistors are used to realize wide impedance matching of the proposed absorber with free space. In Fig. 4, it is observed that the depths of reflection coefficient within the whole bandwidth varies with the different values of the resistor R_r. Here, a

This article has been accepted for publication in a future issue of this journal, but has not been fully edited. Content may change prior to final publication. Citation information: DOI 10.1109/LAWP.2019.2895971, IEEE Antennas and Wireless Propagation Letters

relatively optimal resistor value (R_r = 120 ohms) is selected, where the reflection coefficient of the proposed absorber is below -18 dB from 5.2 to 13.8 GHz. In other words, less than 1.6% power is reflected when EM wave impinges into it. Then, the other parameter l_f is also tuned to evaluate the performance of the proposed absorber, as shown in Fig. 4 as well. It is found that the depths of the reflection coefficients are also sensitive to l_f, and l_f = 4.5 mm is selected to obtain the optimal reflection coefficient (which is better than -18 dB from 5.2 to 13.8 GHz). The input impedance (I-IM) of the dual-polarized and wideband absorber is also plotted in Fig. 4. It is deduced that it can be matched with 120π in a wide frequency band.

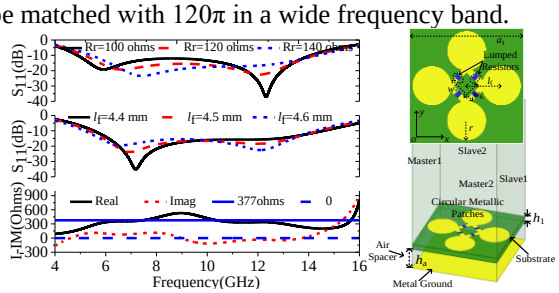

Fig.4. The reflection coefficient and input impedance of the dual-polarization, and wideband absorber with different values of R_r and l_f.

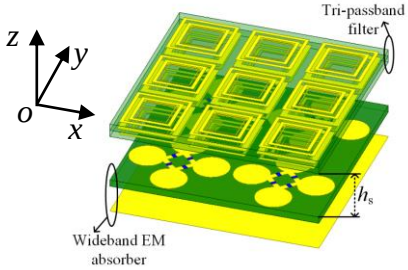

Fig.5. Geometry of the proposed triple-band absorber with wide absorption bandwidths.

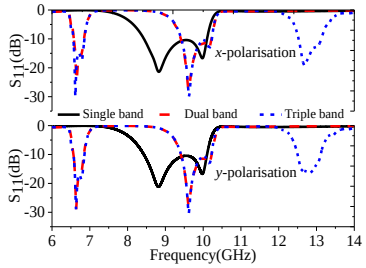

Fig.6. Simulated reflection coefficients of the proposed single/dual/triple-band absorber.

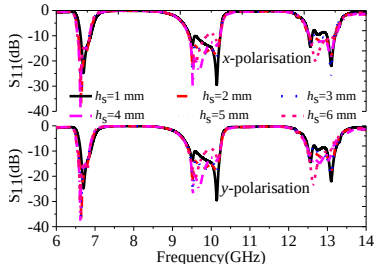

Fig.7. Simulated reflection coefficients of the proposed triple-band absorber with relatively wide absorption bandwidths under different values of h_s.

C. *Triple-band absorber with wide absorption bandwidths*

The absorber in Section II-A gives very wide absorption bandwidth. However, in some applications (e.g., in [13] [14]), we only need the absorption at certain frequencies to pure the frequency spectrum instead of the whole band. The existing triple band absorbers have extremely narrow absorption bandwidths. In this subsection, a triple band absorber with a wide absorption bandwidth is designed to solve this problem.

The proposed triple-band absorber is constructed by cascading the triple-band bandpass filter and the wideband absorber. In theory, the triple-band bandpass filter can be attached on the wideband absorber seamlessly and directly. However, the implementation of the wideband structure is metallic structure, therefore, a separation h_s is unavoidable as shown in Fig. 5. Then, the S_{11} of the single/ dual/triple-band absorber is simulated in *x*- and *y*-polarisation as shown in Fig. 6 (a). Compared with Fig. 2, the S_{11} of the single-/ dual-/ triple-band absorbers are in high accordance with these of the corresponding bandpass filters. In addition, since the proposed absorbers are dual-polarized, the results will be the same when the incident wave is +/- 45-degree polarized.

Here, the absorption performance of the proposed triple-band absorber is further investigated. The separation h_s is a key parameter as it determines the entire thickness of the proposed triple-band absorber. The separation h_s is therefore varied to observe its impact on the S_{11} of the proposed triple-band absorber. It can be predicted that the S_{11} may be deteriorated when the h_s is small since the electromagnetic interferences between the wideband absorber and bandpass FSS filter are stronger. Fig. 6 (b) gives the S_{11} of the triple-band absorber under different separation h_s. Even when the separation h_s is equal to 1 mm, the wide absorption bandwidths of the proposed triple-band absorber are still observed, which indicates the total thickness of the triple band absorber can be further reduced.

Table I. Parameters of the triple-band bandpass filter and wideband absorber. (unit: mm)

a	h	l	l_1	l_2	l_3	w
10	1	8	6.2	4.4	8.5	0.5
w_1	w_2	w_3	d	d_1	d_2	d_3
0.5	0.12	0.9	1	0.4	0.4	0.75
a_1	ha	h_1	r	l_f	w_4	w_5
15	3	1	2.6	4.5	2.4	4.0

III. Experimental Measurement

In this section, the triple-band FSS bandpass filter and the wideband absorber with the optimal dimensions as listed in Table I, are fabricated using the standard printed circuit board (PCB) technology.

Fig. 8 (a) and (b) shows the photographs of the fabricated triple-band bandpass FSS filter and wideband absorber. Eight screws are used to attach the two layers of bandpass filter tightly. The wideband absorber is assembled by using eight plastic posts with the same height of 3 mm to fix the upper layer and metal ground. Two standard horn antennas with the operating frequencies from 2 to 18 GHz are used as the transmitting and receiving antennas to measure the S_{21} of the triple-band bandpass filter, as illustrated in Fig. 8 (c). A vector network analyzer (Agilent N5244A) is used for data processing. The distance between the antennas and the triple-band bandpass filter is adopted to ensure a measurement at far field condition. Fig. 9 (a) compares the measured and simulated S_{21}

This article has been accepted for publication in a future issue of this journal, but has not been fully edited. Content may change prior to final publication. Citation information: DOI 10.1109/LAWP.2019.2895971, IEEE Antennas and Wireless Propagation Letters

of the triple-band bandpass filter in *x*- and *y*-polarization. Three passbands are marked with shadows. It is observed that the measured results of the second and third passbands are highly consistent with that of the simulated ones. There exists a frequency discrepancy for the first passband as the fabricated sample is relatively small compared to the wavelength at around 6.8 GHz, and the beam width of the transmitting and receiving horn antennas are relatively wide at 6.8 GHz to cause the measurement tolerances. Fig. 9 (b) compares the measured and simulated S_{11} of the wideband absorber in *x*- and *y*-polarization. It is observed that the simulated and measured results are in a good agreement from 6 to 14.5 GHz.

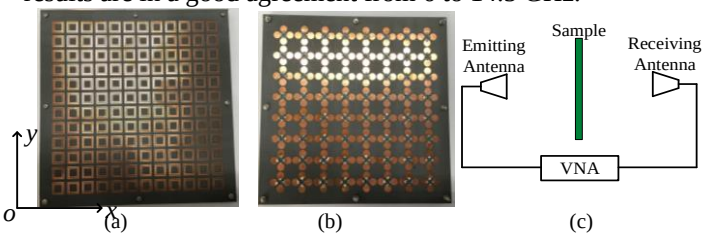

Fig. 8. Photographs. (a). Triple-band bandpass FSS filter, (b). Wideband absorber. (c). Measurement setup for the triple-band bandpass filter.

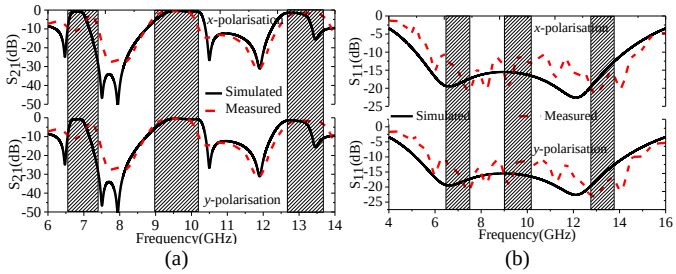

Fig. 9. Measured and simulated S-parameter. (a). Triple band bandpass FSS filter. (b). Wideband absorber.

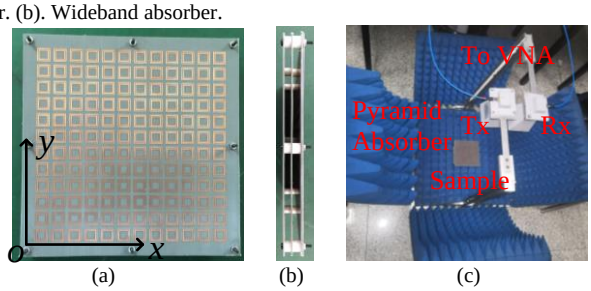

Fig. 10. The photographs of the triple-band absorber. (a) Front view, (b) Side view. (c). Measurement setup.

After measuring the triple-band bandpass FSS filter and wideband absorber, we assemble them together to establish the proposed triple-band absorber, as given in Fig.10 (a) and (b). Here, the separation *h*s=4 mm is selected, so the entire thickness of the absorber is 9 mm (around 0.20 λ at the lower absorption frequency). Then, the S_{11} of the triple-band absorber are all measured in *x*- and *y*-polarisation under normal incidence as presented in Fig. 11, where the simulated results are also plotted for comparison. The measurement setup is shown in Fig. 10 (c). The discrepancies are attributed to the fabrication and measurement tolerances. The absorption performance of the triple-band absorber is also measured and discussed under oblique incidence. By simultaneously rotating the transmitting and receiving horn antennas away from the normal direction as outlined in [13], the reflection coefficients of the triple-band absorber are measured at different transverse electric (TE) and transverse magnetic (TM) polarization incident angles, respectively. Fig. 12 presents the measured results under TE and TM polarization waves with different oblique incidence angles. The three absorption bands are still maintained when the incident angle varies from 0° to 30° for TE and TM oblique incidence waves, with the relatively wide absorption bands.

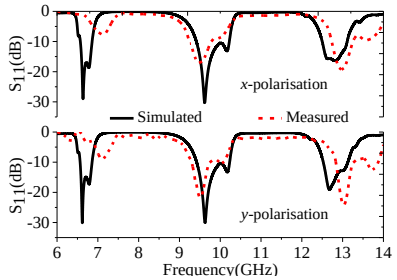

Fig. 11. Measured and simulated reflection coefficient of the triple-band absorber in *x*- and *y*-polarizations.

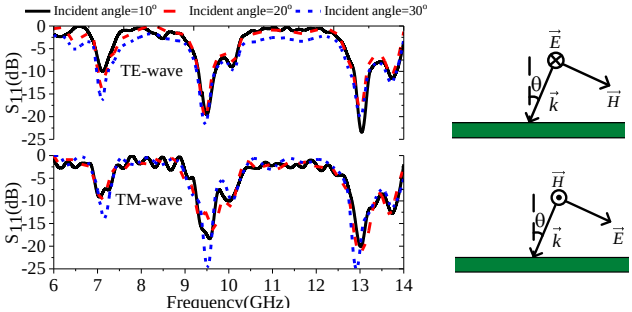

Fig. 12. Measured reflection coefficient of the triple-band absorber under oblique incidence.

At last, the performance comparisons between our proposed absorber and the related work are shown in Table II. Although the thickness of our work is a little thick, the absorption bandwidths are significantly wide. Moreover, as the simulations demonstrated, the separation h_s can be reduced into 1mm in our design. If the profile of the wideband absorber can be lower, the thickness of the proposed absorber would significantly be decreased accordingly. In addition, from our studies, the multi-band absorption bandwidths in [8]-[10] are difficult to broaden by just increasing the supporting substrate thickness.

Table II. Performance comparisons with other related work

Refs.	Order	RAB (%)	CF (GHz)	Profile
[8]	1	0.5, 0.8, 0.9	4.19, 9.34, 11.48	Single layer
[9]	1	0.6, 1.2, 1.1	3.25, 9.45, 10.90	Single layer
[10]	1	0.5, 0.6, 1.1	4.02, 6.75, 9.24	Single layer
This work	2	5.2, 8.0, 6.4	6.88, 9.51, 12.85	Multilayer

Order: number of reflection zeros in every absorption band; RAB: relative absorption bandwidth; CF: center frequency in every absorption band.

IV. Conclusion

Multi-band absorbers with wide absorption bandwidths are proposed based on impedance matching theory. The proposed triple-band absorber is established by cascading the triple-band bandpass FSS filter and the wideband absorber, and then is fabricated and measured. Good agreements are observed between the simulated and measured results. The proposed design provides an alternative method for multi-band absorber with desired absorption performance.

REFERENCES

[1] N. I. Landy, S. Sajuyibge, J. J. Mock, D. R. Smith, and W. J. Padilla, "Perfect metamaterial absorber", *Phys. Rev. Lett.*, vol. 100, no. 20, May 2008.

[2] Y. Shang, Z. Shen, and S. Xiao, "On the design of single-layer circuit analog absorber using double-loop array", *IEEE Trans. Antennas Propag.*, vol. 61, no. 12, pp. 6022-6029, Dec. 2013.

[3] X. Lin, P. Mei, P. Zhang, Z. Chen, and Y. Fan, "Development of a resistor-loaded ultra-wideband absorber with antenna reciprocity", *IEEE Trans. Antennas Propag.*, vol. 64, no. 11, pp. 4910-4913, Nov. 2016.

[4] N. Zabri, R. Cahill, and A. Schuchinsky., "Polarization independent resistively loaded frequency selective surface absorber with optimum oblique incidence performance", *IET Microw. Antenna Propag.*, vol. 8, no. 14, pp. 1198-1203, 2014.

[5] D. Chaurasiya, *et al*., "Compact multi-band polarization-insensitive metamaterial absorber", *IET Microw. Antenna Propag*., vol. 10, no. 1, pp. 94-101, 2016.

[6] M. Agarwal, A. Behera, and M. Meshram, "Wide-angle quad-band polarization-insensitive metamaterial absorber", *Electron Lett*., vol. 52, no. 5, pp. 340-342, 2016.

[7] S. Ghosh, S. Bhattacharyya, and D. Chaurasiya, "polarization-insensitive and wide-angle multi-layer metamaterial absorber with variable bandwidths", *Electron Lett*., vol. 51, no. 14, pp. 1050-1052, 2015.

[8] N. Mishra, D. Choudhary, R. Chowdhury, K. Kumari, and R. Chaudhary, "An investigation on compact untr-thin triple band polarization independent metamaterial absorber for microwave frequency application," *IEEE Access*, vol. 5, pp. 4370-4376, 2017.

[9] H. Zhai, C. Zhan, Z. Li, and C. Liang, "A triple-band ultrathin metamaterial absorber with wide-angle and polarization stability", *IEEE Antennas Wireless Propag Lett.*, vol. 14, pp. 241-244, 2015.

[10] X. Shen, T. Cui, J. Zhao, H. Ma, W. Jiang, and H. Li, "Polarization-independent wide-angle triple-band metamaterial absorber," *Opt. Express*, vol. 19, no. 10, pp. 9401-9407 (2011).

[11] N. Wang, J. Tong, W. Zhou, W. Jiang, and J. Li, "Novel quadruple-band microwave metamaterial absorber", *IEEE Photonic Journal*, vol. 7, no. 1, Feb 2015.

[12] S. Bhattacharyya, and S. Ghosh, "Triple band polarization-independent metamaterial absorber with bandwidth enhancement at X-band", *J. Appl. Phys*., vol. 114, no. 9, p. 094514, 2013.

[13] P. Mei, X. Lin, J. Yu, A. Boukarkar, P. Zhang, and Z. Yang, "Development of a low radar cross section antenna with band-notched absorber," *IEEE Trans on Antennas and Propag*., vol. 66, no. 2, pp. 582-589, Feb 2018.

[14] H. Huang, and Z. Shen, "3-D absorptive frequency selective reflector for antenna radar cross section reduction," *IEEE Trans Antennas Propag*., vol. 65, no. 11, pp. 5908-5917, Nov 2017.

[15] C. Jin, Q. Lv, J. Wang and Y. Li., "Capped dielectric inserted perforated metallic plate bandpass frequency selective surface," *IEEE Trans Antennas Propag*., vol. 65, no. 12, pp. 7129-7136, Dec 2017.

[16] B. Li and Z. Shen, "Synthesis of quasi-elliptic bandpass frequency-selective surface using cascaded loop arrays," *IEEE Trans Antennas Propag*., vol. 61, no. 6, pp. 3053-3058, June 2013.